

1 **Multi-pass Nanofiltration for Lithium Separation with High**
2 **Selectivity and Recovery**

4 Revised Manuscript Submitted to

6 ***Environmental Science & Technology***

8 *As a Research Article*

10 Aug 2023

12 Ruoyu Wang^a, Rayan Alghanayem^b, and Shihong Lin* ^{a,b}

14 ^aDepartment of Civil and Environmental Engineering, Vanderbilt University, Nashville, Tennessee
15 37235-1831, USA

17 ^b Department of Chemical and Biomolecular Engineering, Vanderbilt University, Nashville,
18 Tennessee 37235-1831, USA

20 *Email: shihong.lin@vanderbilt.edu

22 **ABSTRACT**

23 Nanofiltration (NF) is a promising and sustainable process to extract Li^+ from brine lakes with
24 high Mg^{2+} to Li^+ mass ratios. However, a tradeoff between Li/Mg selectivity and Li recovery exists
25 at the process-scale, and the Li/Mg selectivity of commercially and lab-made NF membranes in a
26 single-pass NF process is insufficient to achieve the industrially required Li purity. To overcome
27 this challenge, we propose a multi-pass NF process with brine recirculation to achieve high
28 selectivity without sacrificing Li recovery. We experimentally demonstrate that Li/Mg selectivity
29 of a three-pass NF process with a commercial NF membrane can exceed 1,000, despite the
30 compromised Li recovery due to co-existing cations. Our theoretical analysis further predicts that
31 a four-pass NF process with brine recirculation can simultaneously achieve an ultra-high Li/Mg
32 selectivity of over 4,500 and a Li recovery of over 95%. This proposed process could potentially
33 facilitate efficient NF-based solute-solute separations of all kinds and contribute to the
34 development of novel membrane-based separation technologies.

35

36

37

38

39

40 **KEYWORDS:** nanofiltration, lithium extraction, selective separation, solute-solute separation

41 **SYNOPSIS**

42 Multi-pass nanofiltration with brine circulation using commercial membranes can achieve
43 exceptional performance in lithium-magnesium separation with high selectivity and lithium
44 recovery.

45

46 **INTRODUCTION**

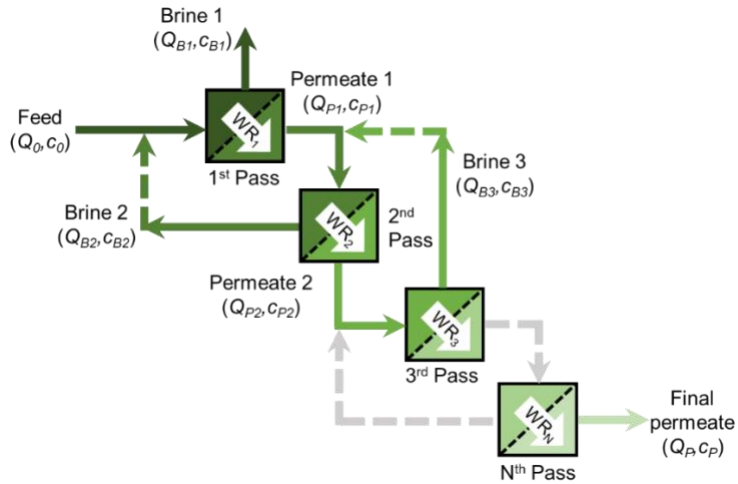
47 Lithium (Li) has become one of the most valuable resources in the 21st century with a sharp
48 increase in demand due to its applications in battery for electrifying transportation and sustainable
49 energy-storage.^{1,2} Li⁺ is abundant in salt lake brine, though at a relatively low concentration
50 compared to other co-existing cations, especially magnesium (Mg), which often exists at a
51 concentration one to three orders of magnitude higher than Li.³ In a typical treatment train for Li
52 extraction (from brine), Li⁺ is recovered at the final precipitation step in the form of hydroxide or
53 carbonate compounds. Because Mg(OH)₂ or MgCO₃ also has low solubility and will thus co-
54 precipitate (with LiOH or Li₂CO₃), separating Li⁺ from Mg²⁺ in previous steps is critical to
55 achieving a final product with high purity. Conventional solar evaporation/precipitation-based Li
56 extraction process requires a large footprint and substantial use of chemicals and cannot effectively
57 handle brines with high Mg²⁺ to Li⁺ mass ratio (MLR).^{2,4} Nanofiltration (NF), which can separate
58 monovalent and divalent ions, has been explored for Li/Mg separation due to its separation
59 effectiveness, modularity, and process sustainability.⁵ As direct lithium extraction is challenging
60 for NF due to the high ionic strength, complex feed composition and high scaling potential, NF is
61 typically integrated with other pre- and post-treatment unit processes to assemble a complete
62 treatment train. Sodium and potassium precipitation (e.g., KCl fertilizer production) and Li-
63 selective adsorption are typical pre-treatment units preceding NF, during which Li is pre-enriched
64 from the original brine lakes. Reverse osmosis can be applied as a post-treatment to concentrate
65 the Li-enriched stream from NF permeate for the final precipitation step and recover the water for
66 next-cycle dilution of brine before it enters the NF process.

67 NF membranes have sub-nanometer pores and charged functional groups that allow them
68 to selectively exclude ions by steric, dielectric, Donnan exclusions, and dehydration mechanisms.
69 The selectivity of monovalent and divalent ions stems from the difference in ion size, valence, and
70 mobility. The Li/Mg selectivity of most commercial and lab-made NF membranes is typically
71 lower than 30, with some exceptional membranes achieving 80~100.⁶⁻¹² Such a selectivity
72 corresponds to a Li purity (i.e., mass ratio of Li over the sum of Li and Mg in the permeate) of
73 10%~90% when treating a typical brine with high MLR (e.g., 10~120) in a single pass of filtration,
74 which fails to meet the industrial requirements of Li product purity (e.g., 98%~99.9%) without
75 additional chemical purification.

76 While the membrane's intrinsic ability to separate Li^+ and Mg^{2+} may be substantially
77 improved with a better design of membrane material and structure (e.g., incorporating coordination
78 chemistry),^{7,12-15} an operational tradeoff always exists at the process scale between the two success
79 criteria for Li extraction in a single-pass NF process: Li/Mg selectivity and Li recovery.¹⁶
80 Specifically, selectivity inevitably decreases as more Li^+ is recovered.¹⁶ Therefore, innovation and
81 optimization of the current NF-based Li/Mg separation process are necessary to improve both
82 Li/Mg selectivity (i.e., product purity) and Li recovery simultaneously, regardless of the intrinsic
83 membrane performance.

84 Multi-pass filtration is an effective strategy to improve water purity in water treatment
85 processes.¹⁷ Two-pass or even three-pass reverse osmosis has been adopted in seawater
86 desalination and wastewater purification as the feed streams contain small and neutral compounds
87 (e.g., boron and some micropollutants) that cannot be sufficiently rejected in a single pass.^{18,19}
88 Similarly, a multi-pass NF process, where the permeate in each pass is repressurized to feed into
89 the next pass (Figure 1), is hypothesized to achieve higher Li/Mg selectivity by rejecting the less
90 permeable ion, Mg^{2+} , for multiple times. Similar approach has been employed in selective
91 electrodialysis for Li/Mg separation. A four-stage electrodialysis module was validated
92 experimentally to enhance the Li/Mg selectivity by orders of magnitude.²⁰

93 However, the overall Li recovery can be compromised in a multi-pass NF process if the
94 brines are disposed directly after each filtration pass, as achieving 100% water recovery or Li
95 recovery is unlikely in any single pass. To address this issue, the brine of each pass beyond the 1st
96 pass may cycle back to the previous pass to be part of its feed solution (dash arrows in Figure 1).
97 With recirculation, the multi-pass process has only one main brine stream from the 1st pass, and
98 one main permeate stream (i.e., product stream) from the last pass, thereby mitigating the loss of
99 Li^+ in the process.



100

101 **Fig. 1 Schematics of the multi-pass NF process for Li/Mg separation.** The permeate of N^{th} pass is the
 102 feed of $(N+1)^{\text{th}}$ pass. The brine of N^{th} pass recirculates back to the feed of $(N-1)^{\text{th}}$ pass. Each pass can be
 103 operated at different pressures and water recovery. Passes between the 3^{rd} and N^{th} pass, and pumps for
 104 pressurizing streams and recirculation are omitted for simplicity.

105 In this study, we first conduct experiments to evaluate the Li/Mg separation performance
 106 of a three-pass NF process without brine recirculation under varying operating pressures, using a
 107 simple Li/Mg mixture as the feed solution. We then investigate the impacts of co-existing cations
 108 and anions on Li/Mg selectivity and Li recovery of the multi-pass process. Finally, we extend the
 109 analysis to predicting the performance of multi-pass Li/Mg separation with brine recirculation by
 110 applying a module-scale NF model.

111

112 MATERIALS AND METHODS

113 Experiments of multi-pass NF without brine recirculation

114 Multi-pass Li/Mg NF separation experiments without brine recirculation were carried out using a
 115 commercial spiral-wound NF membrane module with polyamide membrane, NFX-1812 (Synder
 116 Filtration, USA, Table S1), in a crossflow filtration system. NFX membrane was selected in this
 117 study over other more commonly seen commercial NF membranes (e.g., NF270 and NF90 from
 118 Dupont) because NFX membrane is closer to the upper bound in the material tradeoff plot (Li/Mg
 119 permeability ratio vs Li/water permeability ratio),¹⁶ which suggests NFX has potential to achieve
 120 moderate purity and Li recovery at the same time. The effective membrane area of the module is
 121 0.37 m². Pure water permeability was first measured after pre-compaction of the membrane. Li/Mg
 122 separation was then conducted with synthetic brines at different pressures in a batch mode, i.e.,

123 circulating the brine stream back to the feed tank and collecting the permeate stream in a separate
124 tank until the target water recovery was achieved. The target water recovery was set as 75% for
125 the 1st pass (unless otherwise stated) to avoid a very low water flux at higher water recovery, as a
126 low flux requires more membrane area in the real process to achieve the same target water recovery.
127 The target water recovery was set as 85% for the 2nd and 3rd passes (unless otherwise stated), which
128 was possible because the osmotic pressures for the 2nd and 3rd passes were much lower than that
129 of the 1st pass. The determination of water recovery considers the solution dead volume in the
130 membrane module and in the crossflow filtration loop. A balance was used to monitor the mass
131 increase of permeate tank over time for water recovery estimation. In the batch mode where the
132 water recovery of the small membrane coupon in each pass is negligible, the spatial variation of
133 feed concentration in a real membrane module is mimicked by the temporal variation of feed
134 concentration in the feed tank.

135 We focus the application scenario of NF on treating “old brines” (i.e., the brine after K and
136 Na precipitation) or the elution solutions after a Li-selective adsorption pre-treatment step.
137 Specifically, a simple mixture of 3.4 mM LiCl and 19.6 mM MgCl₂ was first used as the initial
138 feed solution to evaluate multi-pass separation performance. The concentrations of Li⁺ (23.8 mg
139 L⁻¹) and Mg²⁺ (470.4 mg L⁻¹) represent a diluted brine with a MLR of 20. We note that the dilution
140 of feed solution is typically necessary for two reasons: (1) to reduce the osmotic pressure so that a
141 relatively low operating pressure can be used; and (2) to reduce the charge screening effect so that
142 the Donnan effect can be leveraged for the selective separation of monovalent and divalent cations.
143 We also note that the fresh water used for dilution can be recouped in the subsequent RO post-
144 treatment for concentrating the NF permeate. The determination of the optimal dilution factor is
145 beyond the scope of this study and requires more comprehensive analysis to account for separation
146 performance, process cost, and the availability of fresh water to initiate the process.

147 Two more complex and practical brine compositions (Table S2) were then tested to study
148 the impacts of co-existing cations and anions on the multi-pass Li/Mg separation. Feed and
149 permeate solutions were sampled at different water recovery values with a sampling volume of 1
150 mL per sample. The permeate flowing out of the spiral-wound module (before entering the
151 permeate tank) and the permeate in the permeate tank (where permeate effluent mixes with existing
152 solution in the tank) were sampled separately and were referred to as the ‘local permeate’ and

153 ‘cumulative permeate’, respectively. Cation concentrations of collected samples were measured
154 by inductively coupled plasma optical emission spectroscopy. Anion concentrations were
155 measured by ion chromatography. For multi-pass filtration experiments without recirculation, each
156 pass was conducted sequentially with the permeate composition used as the feed composition for
157 the next pass.

158 The local permeate flux, J_w , at different water recovery was determined using the following
159 equation:

$$J_w = \frac{\Delta m}{A\Delta t} \quad (1)$$

160 where Δm is the permeate tank mass change in a short time interval of Δt and A is the effective
161 filtration area of the membrane module. The observed local ion rejection at a certain water recovery
162 (WR), $R_i^{\text{loc}}(WR)$, was calcualted as

$$R_i^{\text{loc}}(WR) = 1 - \frac{c_{\text{p},i}^{\text{loc}}(WR)}{c_{\text{b},i}(WR)} \quad (2)$$

163 where $c_{\text{p},i}^{\text{loc}}$ and $c_{\text{b},i}$ are concentrations of the target ion in the local permeate (sampled at the outlet
164 of the permeate tube) and brine (a.k.a. retentate), respectively. While the cumulative ion rejection,
165 R_i^{cum} , was calcualted as

$$R_i^{\text{cum}}(WR) = 1 - \frac{c_{\text{p},i}^{\text{cum}}(WR)}{c_{\text{f},i}} \quad (3)$$

166 where $c_{\text{p},i}^{\text{cum}}$ is the concentration of the target ion in the cumulative permeate (sampled in the
167 permeate tank), and $c_{\text{f},i}$ is the initial feed concentration of the current pass. The cumulative Li/Mg
168 selectivity or separation factor, $S_{\text{Li/Mg}}$, is defined as²¹

$$S_{\text{Li/Mg}} \equiv \frac{1 - R_{\text{Li}}^{\text{cum}}}{1 - R_{\text{Mg}}^{\text{cum}}} \quad (4)$$

169 Li purity (η_{Li}) is related to the MLR of the feed solution and the Li/Mg selectivity via the following
170 equation:

$$\eta_{\text{Li}} = \frac{1}{1 + \text{MLR}/S_{\text{Li/Mg}}} \quad (5)$$

171 Li recovery (*LiR*), defined as the mass fraction of Li^+ in the feed that is eventually recovered in
 172 the permeate, can be quantified by

$$LiR = WR(1 - R_{\text{Li}}^{\text{cum}}) \quad (6)$$

173 We note that $S_{\text{Li/Mg}}$ (or η_{Li}) and *LiR* are both important performance metrics and a successful
 174 Li/Mg separation must achieve high $S_{\text{Li/Mg}}$ and *LiR* simultaneously.¹⁶

175

176 **Modeling multi-pass NF with brine recirculation**

177 To validate multi-pass NF without brine recirculation, each filtration pass was conducted
 178 separately using a benchtop filtration system in the batch mode, as described in the previous section.
 179 However, for the validation of multi-pass NF with brine recirculation, a pilot-scale system is
 180 required, where a high value of water recovery can be achieved in a single pass, and the brine from
 181 each pass is recirculated to the feed of the previous pass to achieve steady-state operation.
 182 Therefore, in this study (without access to a pilot scale system), the performance of multi-pass NF
 183 with brine recirculation was simulated using a modeling approach.

184 A module-scale NF model for mixture solutions was applied to evaluate the Li/Mg
 185 separation performance of the multi-pass NF process, in which the local mass transport across the
 186 membrane was described by the solution diffusion electromigration model (SDEM) as described
 187 in the Supporting Information (Text S1).²²⁻²⁴ For multi-pass filtration without brine recirculation,
 188 each pass can be solved sequentially with the permeate composition of one pass used as the feed
 189 to the next pass. For multi-pass filtration with brine recirculation, the feed of each pass between
 190 the 1st and the last pass (i.e., 2nd to (N-1)th pass) is a mixture of the permeate from the previous
 191 pass and the brine from the next pass (Figure 1). When steady state operation is achieved, the mass
 192 balance of water can be described as

$$Q_n = \begin{cases} Q_0 + Q_2(1 - WR_2), & \text{for } n = 1 \\ Q_{n-1}WR_{n-1} + Q_{n+1}(1 - WR_{n+1}), & \text{for } n = 2 \sim N - 1 \\ Q_{n-1}WR_{n-1}, & \text{for } n = N \end{cases} \quad (7)$$

193 where N is number of passes, Q_n and WR_n are the feed flow rate and water recovery of pass n ,
194 respectively, Q_0 is the initial feed flow rate. Q_n is a function of Q_0 and water recovery of each pass
195 and can be solved analytically. The mass balance of ions can be described as

$$c_{f,n} = \begin{cases} Q_0 c_0 + Q_2 (1 - WR_2) c_{b,2}, & \text{for } n = 1 \\ Q_{n-1} WR_{n-1} c_{p,n-1} + Q_{n+1} (1 - WR_{n+1}) c_{b,n+1}, & \text{for } n = 2 \sim N - 1 \\ c_{p,n-1}, & \text{for } n = N \end{cases} \quad (8)$$

196 where $c_{f,n}$, $c_{p,n}$, and $c_{b,n}$ are feed, permeate, and brine concentrations of pass n , respectively. $c_{f,n}$
197 depends on both $c_{p,n-1}$ and $c_{b,n+1}$, and is thus solved iteratively until the steady state is found. The
198 module-scale NF model was first validated by comparing predictions to the experimental results
199 of multi-pass NF without recirculation. The analysis was then extended to the multi-pass system
200 with recirculation for different numbers of passes.

201

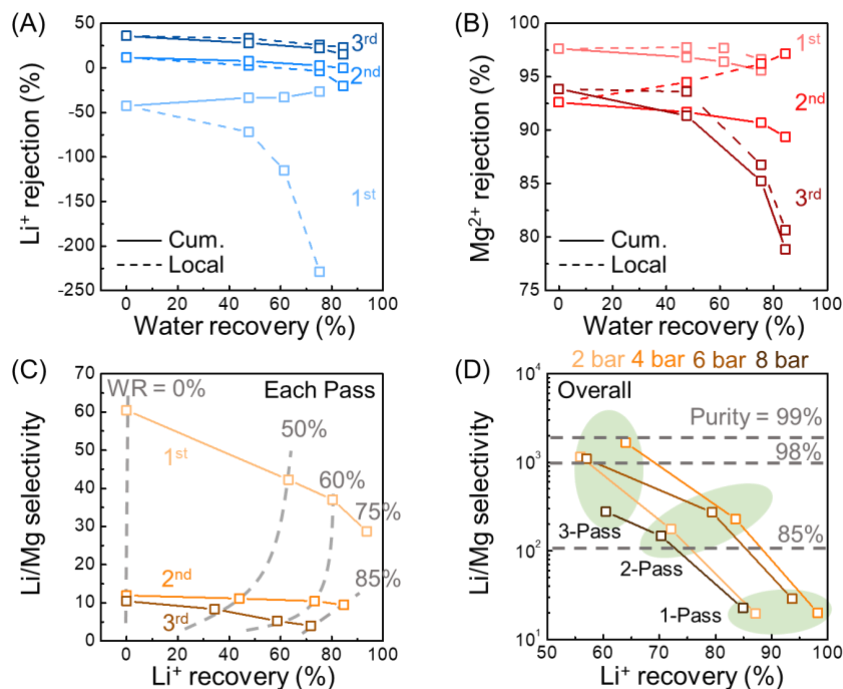
202 RESULTS AND DISCUSSION

203 **Tradeoff between selectivity and recovery in multi-pass Li/Mg separation without 204 brine recirculation**

205 Li/Mg separation performance of a three-pass NF process without recirculation was first tested
206 with the simple Li/Mg feed without other cation species. Both cumulative and local Li^+ rejections
207 increase with number of passes, while Mg^{2+} rejections decrease (Figure 2A and 2B). Negative
208 rejection of Li^+ is common in NF with mixed-salt feed solution as a result of maintaining Donnan
209 equilibrium when the feed solution is abundant in the strongly rejected Mg^{2+} while Cl^- can easily
210 permeate through the membrane.²⁴⁻²⁶ The permeation of Cl^- promotes the transport of Li^+ to
211 maintain charge neutrality in the permeate. The local Li^+ rejection in the 1st pass can be strongly
212 negative when water recovery increases (Figure 2A), mainly due to both the increasing local MLR
213 and decreasing local water flux (Figure S1) as the driving force diminishes with the increasing
214 brine osmotic pressure. Li^+ rejection becomes positive in the 2nd pass and further increases in the
215 3rd pass as most Mg^{2+} is rejected in the 1st pass. The MLR of the feed solution (which is the
216 permeate of the last pass, except for the 1st pass) drops by an order of magnitude after each pass
217 (Figure S2).

218 NFX membrane has slightly negative charges near neutral pH (e.g., isoelectric point around
219 pH 5). A recent study has shown that the adsorption of multivalent cations (e.g., Mg^{2+}) to

220 carboxylic functional groups may lead to charge reversal, i.e., the membrane may become
 221 positively charged,²⁷ which in turn benefits the rejection of Mg^{2+} and thus increases Li/Mg
 222 selectivity. With substantially reduced Mg^{2+} concentrations in feed solutions of the 2nd and 3rd
 223 passes (Figure S2), the charge reversal effect may be weakened and thus the membrane becomes
 224 less positively charged, which is a possible explanation of the reduced Mg^{2+} rejection in later
 225 passes. Another possibility is that the Mg^{2+} adsorption is not enough to cause charge reversal so
 226 that the membrane remains negatively charged in later passes. The enhanced Donnan effect due to
 227 the reduced feed ionic strength in later passes leads to the reduced Mg^{2+} rejection.



228

229 **Fig. 2 Performance of a three-pass Li/Mg separation process without brine recirculation.** (A-B) Local
 230 and cumulative Li⁺ rejection (A) and Mg²⁺ rejection (B) as a function of water recovery in each pass. (C)
 231 Li/Mg selectivity versus Li recovery in each pass. Pressure in panels (A-C) was 6 bar. (D) Overall Li/Mg
 232 selectivity and Li recovery variation with number of passes using different pressures. Feed solution was the
 233 simple LiCl/MgCl₂ mixture. Water recovery was 75% for the 1st pass and 85% for the rest.

234 Li/Mg selectivity is sensitive to Mg²⁺ rejection due to how selectivity is defined based on
 235 Eq. 4, especially when Mg²⁺ is well rejected (e.g., $R_{Mg} > 95\%$). Thus, the tradeoff between Li/Mg
 236 selectivity and Li recovery is most obvious in the 1st pass where the selectivity drops from 60 to
 237 less than 30 as Li recovery increases from 0 to over 90% (Figure 2C). The tradeoff still exists in
 238 the 2nd and 3rd passes, although Li/Mg selectivity becomes less sensitive to Li recovery (Figure
 239 2C). The selectivity for the 2nd and 3rd passes (<15) is much lower than that of the 1st pass due to

240 the reduced Mg^{2+} rejection and increased Li^+ rejection caused by roughly an order of magnitude
241 reduction in MLR following each pass. In other words, we can achieve high Li recovery in 2nd and
242 3rd pass without sacrificing too much selectivity in the same pass, even though the selectivity is
243 relatively low compared to that of the 1st pass.

244 The tradeoff between selectivity and recovery is affected by applied pressure or permeate
245 flux (Figure S3). Although a higher pressure allows to achieve a higher water recovery, especially
246 in the 1st pass where the osmotic pressure increases rapidly at high water recovery, the higher water
247 flux resulting from a higher operating pressure can be detrimental to Li recovery: if water
248 permeation is much faster than Li^+ permeation, only a small fraction of Li^+ in the feed solution can
249 be recovered in the permeate.¹⁶

250 According to our recent work, the operating pressure also has a non-monotonic impact on
251 the Li/Mg selectivity.¹⁶ The lower selectivity in the low-pressure range is due to the weakened
252 “dilution effect”: the low water flux reduces the Mg^{2+} rejection to which the Li/Mg selectivity is
253 very sensitive. The lower selectivity in the high-pressure range is a result of enhanced
254 concentration polarization (CP) which increases the MLR at the membrane interface. The optimal
255 pressure or water flux for optimal Li/Mg selectivity depends on both the membrane properties and
256 feed solution composition (and was 4 bar in our case based on the results shown in Figure 2D).
257 Overall, the Li/Mg selectivity exceeds 100 with the two passes for all tested pressure and can even
258 exceed 1,000~2,000 (equivalent to a purity of 98%~99%) with three passes except when 8 bar was
259 applied (Figure 2D). However, the cumulative loss of Li recovery (~40%) is also substantially
260 higher than the single-pass process, which may be mitigated by recovering more water in each
261 pass and by introducing the brine recirculation strategy.

262

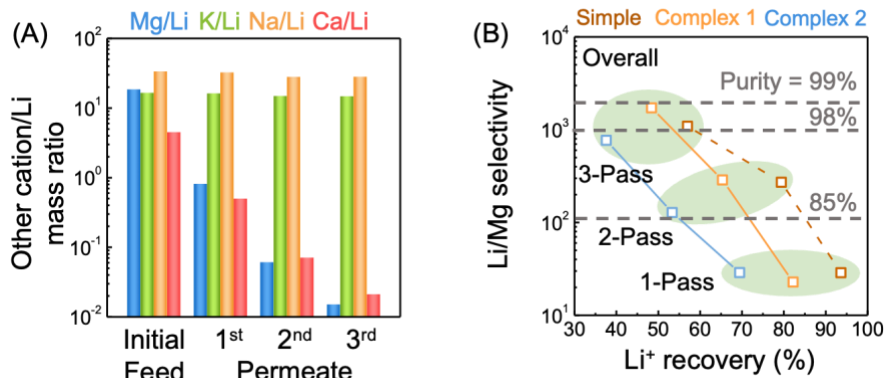
263 **Impacts of co-existing cations and anions on multi-pass Li/Mg separation**

264 Real salt-lake brines are complex multicomponent solutions with high salinities, containing a
265 variety of cations (e.g., Li^+ , Mg^{2+} , Ca^{2+} , K^+ and Na^+ , etc.), in contrast to the simple dual cation
266 feed solution with only LiCl and MgCl₂ as used in most prior studies. The presence of Ca^{2+} in the
267 permeate of NF process would directly deteriorate the product purity as $CaCO_3$ is insoluble. While
268 the presence of K^+ and Na^+ is less harmful to the Li purity, it can still compromise Li recovery due

269 to competitive transport in the NF process. Furthermore, the existence of other cations also changes
270 the rejections of Li^+ and Mg^{2+} as compared to that in a simple Li/Mg feed, ultimately impacting
271 the Li/Mg selectivity and Li recovery. A mixture of LiCl , MgCl_2 , CaCl_2 , KCl , and NaCl (complex
272 1 in Table S2) was tested as the feed to validate the effectiveness of multi-pass NF for enhancing
273 Li/Mg selectivity in a more practical scenario. Mg^{2+} shows the highest rejections (85%~95%),
274 while Ca^{2+} rejection is lower but still over 80%. Na^+ and K^+ have similar rejections as Li^+ (Table
275 S3). Both Mg/Li and Ca/Li mass ratio drops by an order of magnitude after each pass, while Na/Li
276 and K/Li mass ratio maintains almost unchanged over the three passes (Figure 3A). Therefore, the
277 NFX membrane is effective to separate monovalent ions from divalent ions, but it shows no
278 selectivity to monovalent cation pairs.

279 The impact of each co-existing cation (e.g., Ca^{2+} , K^+ and Na^+) on the Li/Mg selectivity has
280 been investigated individually in the literature usually at the coupon-scale (i.e., zero water
281 recovery),²⁸ but rarely tested in a mixture and with a high value of water recovery. The existence
282 of Ca^{2+} is reported to increase Li/Mg selectivity,²⁸ as Ca^{2+} usually has a similar rejection as Mg^{2+}
283 which increases the divalent/monovalent cation ratio and thus forces Li^+ rejection to be more
284 negative to balance the transport of Cl^- . Meanwhile, the existence of other monovalent cations,
285 Na^+ or K^+ , is reported to decrease Li/Mg selectivity,²⁸ because both Na^+ and K^+ have a smaller
286 hydrated radius than Li^+ and thus are preferably transferred across the membrane with less
287 hindrance in both interfacial partition and intra-pore transport. When Ca^{2+} , K^+ and Na^+ co-exist in
288 the feed mixture as chloride salts, their opposite individual impacts on Li/Mg selectivity offset
289 each other to some extent, and thus the observed overall Li/Mg selectivity after each pass is similar
290 to, or even higher than, that measured with the simple Li/Mg feed (Figure 3B). The overall Li/Mg
291 selectivity with complex feed 1 approaches 2000 (equivalent to 99% purity) after the 3rd pass.
292 However, Li recovery is further reduced when Ca^{2+} , K^+ and Na^+ co-exist, mainly due to the
293 preferable transport of K^+ and Na^+ over Li^+ . When SO_4^{2-} and Cl^- co-exist as anions (complex feed
294 2 in Table S2), rejections of cations (especially monovalent cations) increased due to the reduced
295 total anion flux as SO_4^{2-} has lower permeance compared to Cl^- . As a result, both Li/Mg selectivity
296 and Li recovery in the three-pass NF process were compromised as compared to the case where
297 SO_4^{2-} was in absence (Figure 3B), consistent with a recent study showing that Li/Mg selectivity in
298 coupon-scale experiments would be overestimated in the absence of SO_4^{2-} .²⁹ The Li-specific
299 energy consumption (SEC_{Li}) of the three-pass NF process without brine recirculation is estimated

300 for the simple feed ($0.23 \text{ kWh mol}^{-1}$), complex feed 1 ($0.30 \text{ kWh mol}^{-1}$), and complex feed 2 ($0.42 \text{ kWh mol}^{-1}$), which increases as less Li was recovered (Table S4).



302

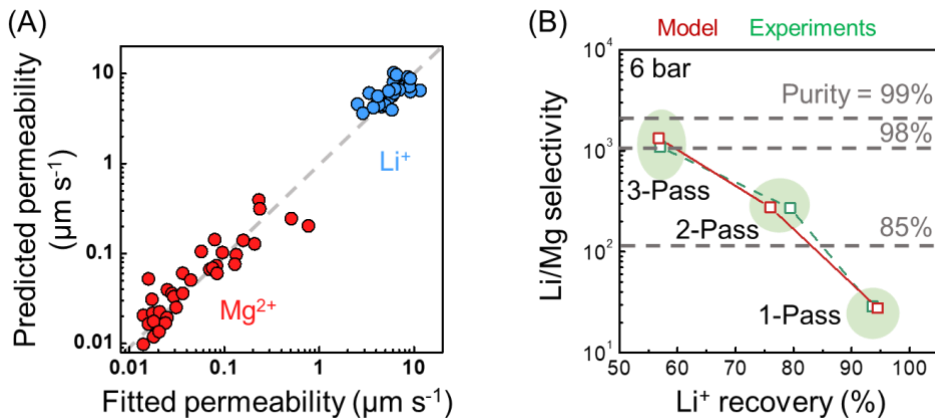
303 **Fig. 3 Impacts of co-existing cations and anions on the performance of a three-pass Li/Mg**
 304 **separation process.** (A) Mass ratio of co-existing cations to Li^+ in the feed and the permeate of each pass.
 305 Results of complex feed 1 (chloride as the only anion) were presented. (B) Overall Li/Mg selectivity and Li
 306 recovery variation with number of passes for simple and complex feed solutions. Complex 1 is sulfate-free
 307 and complex 2 contains sulfate. Water recovery was 75% for the 1st pass and 85% for the rest. Pressure
 308 was 6 bar.

309

310 **High selectivity and recovery achieved simultaneously with brine recirculation**

311 The Li/Mg separation performance of a four-pass NF process with brine recirculation was analyzed
 312 via module-scale modeling. The experimental validation of multi-pass NF with brine recirculation
 313 requires a pilot-scale system where a high value of water recovery can be achieved in a single pass
 314 and was thus not performed in this study due to the lack of access to pilot-test infrastructure. The
 315 local ion transport across the membrane in the module-scale NF model is characterized by ion
 316 permeabilities in the SDEM model. Ion permeability depends on both membrane properties and
 317 solution composition. Experimental results of the three-pass filtration without recirculation were
 318 used to fit Li^+ and Mg^{2+} ion permeabilities under different pressures and water recovery values.
 319 Mg^{2+} permeability increases by over an order of magnitude over the three passes, corresponding
 320 to the rejection reduction from 95% to 80% in Figure 2B, while Li^+ permeability variation is less
 321 substantial (Table S5). An empirical correlation (Eq. S4 and Table S6) successfully captures the
 322 dependence of ion permeability variation on Li^+ and Mg^{2+} concentrations in the brine stream after
 323 accounting for concentration polarization (Figure 4A). The module-scale NF model was then
 324 validated by predicting similar Li/Mg selectivity and Li recovery in a three-pass process without

325 brine recirculation for which we have collected experimental results (Figure 4B, in which the
326 experimental curve is one of the curves reported in Figure 2D).

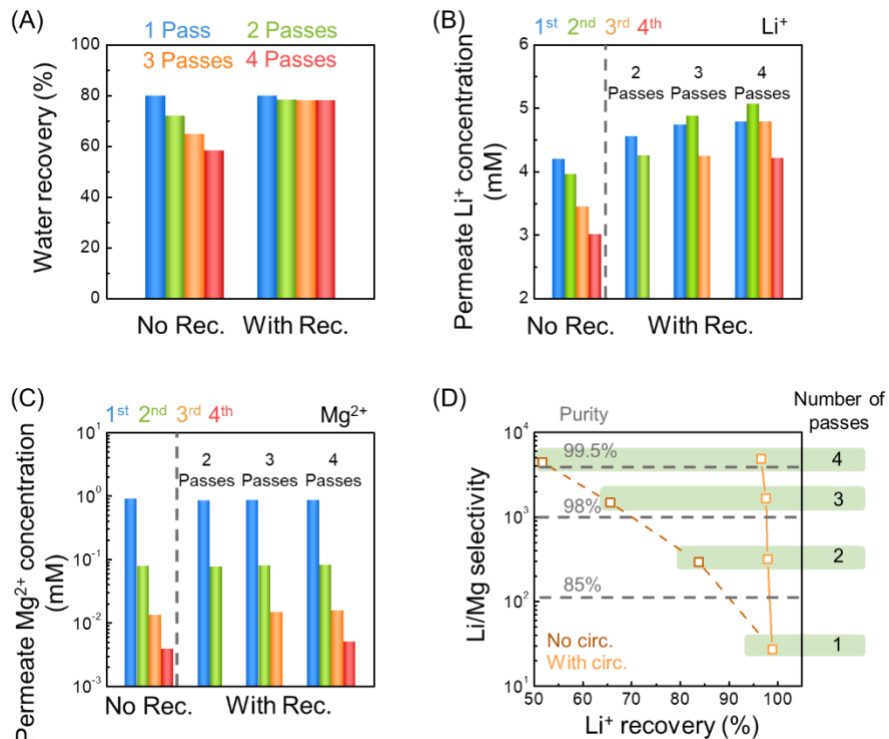


327

328 **Fig. 4 Modeling module-scale performance of Li/Mg separation by NF.** (A) Correlation of predicted and
329 fitted ion permeabilities. Fitted ion permeabilities are from three-pass filtration experiments without
330 recirculation. (B) Validation of the module-scale model by comparing performance predictions of the three-
331 pass filtration process to experimental results. Model used same conditions as the experiments. Feed
332 composition was 3.4 mM LiCl and 19.6 mM MgCl₂, water recovery was 75% for 1st pass and 85% for 2nd
333 and 3rd passes, and pressure was 6 bar.

334 With a validated model that can reasonably predict module-scale performance, the effect
335 of brine recirculation was analyzed. The overall water recovery can maintain at near 80% over
336 four passes when brine is recirculated, while less than 60% of feed water can be recovered without
337 recirculation, which causes substantial Li loss (Figure 5A). With brine recirculation, Li⁺
338 concentrations in the permeate of each pass are higher than those without recirculation (Figure 5B),
339 while Mg²⁺ concentrations in the permeates remain similar (Figure 5C). Our simulation predicts
340 that the Li/Mg selectivity can exceed 4,000 (equivalent to 99.5% purity) with a four-pass filtration
341 without brine recirculation, but at the cost of substantial Li loss of around 15~20% in each pass of
342 the 2nd to 4th passes (dash line in Figure 5D). A high Li/Mg selectivity (4,889) and high Li recovery
343 (96.6%) can be achieved simultaneously with four passes and brine recirculation (solid line in
344 Figure 5D). Thus, the tradeoff between selectivity and recovery can be overcome with brine
345 recirculation. As long as we can achieve high Li recovery in the 1st pass (where brine is not
346 recirculated), the configuration of multi-pass with recirculation can achieve extremely high Li/Mg
347 selectivity while maintaining a high Li recovery. Additionally, the high Li recovery achieved by
348 brine recirculation also results in the reduction of energy consumption from 0.30 kWh mol⁻¹ to
349 0.18 kWh mol⁻¹ in the four-pass NF process (Table S4), though having recirculation adds process

complexity and capital cost. A comprehensive techno-economic analysis is necessary to fairly compare the potential economic benefit of the multi-pass NF process with other different Li/Mg separation technologies after accounting for pre- and post-treatment unit processes in complete Li extraction treatment trains, which is beyond the scope of the current study.



354

355 **Fig. 5 Lithium recovery of multi-pass Li/Mg separation process enhanced by brine recirculation.** (A) Water recovery with and without brine recirculation as a function of number of passes. (B) Li⁺ and (C) Mg²⁺ concentration in the permeate of each pass in the multi-pass NF process with and without brine recirculation. (D) Overall Li/Mg selectivity and Li recovery with and without recirculation as a function of number of passes. Feed solution was the simple LiCl/MgCl₂ mixture. Pressure was 6 bar. Water recovery was set as 80% for the 1st pass and 90% for the rest. Mass transfer coefficient of 100 L m⁻² h⁻¹ was used to account for concentration polarization. The labels "No Rec." and "With Rec." in the x-axis stand for "without brine recirculation" and "with brine recirculation", respectively.

363

364 IMPLICATIONS

365 NF is a promising unit process in the treatment train for extracting Li⁺ from brine lakes with high
 366 mass ratios of Mg²⁺ to Li⁺. However, the Li/Mg selectivity of currently available NF membranes
 367 is not high enough to satisfy the industrial product purity requirements in a single-pass filtration.
 368 Advances in membrane material research may improve the situation but unlikely achieve
 369 satisfactory separation in a single pass. The multi-pass NF process with brine recirculation

370 proposed in this study can achieve ultra-high selectivity without sacrificing Li recovery. The
371 performance may be further enhanced by optimizing the operating pressure and water recovery in
372 each pass, and by applying novel NF membranes with better performance than the tested
373 commercial NF membrane. We note that the feed solution used in this study is relatively dilute
374 (corresponding to a large dilution factor), which shows benefits in separation performance, though
375 from a practical point of view, will require a larger membrane area and a substantial amount of
376 fresh water to initiate the process. Thus, performance of the multi-pass NF with more concentrated
377 feed solutions needs further investigation to evaluate the proper dilution factor considering the
378 potential tradeoff between separation performance and cost. Lastly, although the context of this
379 study is on Li/Mg separation, the technical approach of multi-pass NF with recirculation is
380 expected to be also effective for other types of solute-solute separations in resource extraction and
381 recovery.

382

383 **ASSOCIATED CONTENT**

384 The Supporting Information is available free of charge at: [XXX](#)

385 Module-scale NF model for Li/Mg separation (Text S1); Properties of the commercial NF
386 membrane used in this study(Table S1); Composition of the synthetic brines to study impacts of
387 co-existing cations and anions (Table S2); Rejections of cations in the three-pass Li/Mg separation
388 process (Table S3); Energy consumption of the multi-pass NF process for Li/Mg separation (Table
389 S4); Fitted ion permeability at different concentrations and pressures (Table S5); Linear correlation
390 coefficients for ion permeability (Table S6); Permeate flux at different water recovery under
391 different operating pressures in the 1st pass (Figure S1); Ion mass concentration and MLR in the
392 initial feed, and permeates of each pass (Figure S2); Li/Mg selectivity and Li recovery at different
393 water recovery under different pressures (Figure S3).

394

395 **ACKNOWLEDGEMENT**

396 The authors acknowledge the support from the US National Science Foundation (#2017998, #
397 1903685), Water Research Foundation (Paul L. Busch Award to S.L.), and the US-Israel
398 Binational Agricultural Research and Development Fund (BARD IS-5209-19).

400 **REFERENCES**

401 (1) Choubey, P. K.; Kim, M.; Srivastava, R. R.; Lee, J.; Lee, J. Advance Review on the Exploitation of
402 the Prominent Energy-Storage Element : Lithium . Part I : From Mineral and Brine Resources.
403 *Miner Eng* **2016**, 89, 119–137. <https://doi.org/10.1016/j.mineng.2016.01.010>.

404 (2) Swain, B. Recovery and Recycling of Lithium : A Review. *Sep Purif Technol* **2017**, 172, 388–403.
405 <https://doi.org/10.1016/j.seppur.2016.08.031>.

406 (3) Xu, S.; Song, J.; Bi, Q.; Chen, Q.; Zhang, W.; Qian, Z.; Zhang, L.; Xu, S.; Tang, N.; He, T. Extraction of
407 Lithium from Chinese Salt-Lake Brines by Membranes: Design and Practice. *J Memb Sci* **2021**, 635,
408 119441.

409 (4) Woong, J.; Jun, D.; Thi, K.; Jun, M.; Lim, T.; Tran, T. Hydrometallurgy Recovery of Lithium from
410 Uyuni Salar Brine. *Hydrometallurgy* **2012**, 117–118, 64–70.
411 <https://doi.org/10.1016/j.hydromet.2012.02.008>.

412 (5) Li, X.; Mo, Y.; Qing, W.; Shao, S.; Tang, C. Y.; Li, J. Membrane-Based Technologies for Lithium
413 Recovery from Water Lithium Resources: A Review. *J Memb Sci* **2019**, 591, 117317.
414 <https://doi.org/10.1016/j.memsci.2019.117317>.

415 (6) Xu, P.; Hong, J.; Xu, Z.; Xia, H.; Ni, Q. Novel Aminated Graphene Quantum Dots (GQDs-NH2)-
416 Engineered Nanofiltration Membrane with High Mg²⁺/Li⁺ Separation Efficiency. *Sep Purif
417 Technol* **2021**, 258 (P2), 118042. <https://doi.org/10.1016/j.seppur.2020.118042>.

418 (7) Yang, Z.; Fang, W.; Wang, Z.; Zhang, R.; Zhu, Y. Dual-Skin Layer Nanofiltration Membranes for
419 Highly Selective Li⁺/Mg²⁺ Separation. *J Memb Sci* **2021**, 620, 118862 .

420 (8) Bi, Q.; Zhang, C.; Liu, J.; Liu, X.; Xu, S. Positively Charged Zwitterion-Carbon Nitride Functionalized
421 Nanofiltration Membranes with Excellent Separation Performance of Mg²⁺ / Li⁺ and Good
422 Antifouling Properties. *Sep Purif Technol* **2021**, 257 (August 2020), 117959.
423 <https://doi.org/10.1016/j.seppur.2020.117959>.

424 (9) Xu, P.; Hong, J.; Qian, X.; Xu, Z.; Xia, H.; Ni, Q. “Bridge” Graphene Oxide Modified Positive
425 Charged Nanofiltration Thin Membrane with High Efficiency for Mg²⁺/Li⁺ Separation.
426 *Desalination* **2020**, 488 (March). <https://doi.org/10.1016/j.desal.2020.114522>.

427 (10) Shen, Q.; Xu, S.; Xu, Z.-L.; Zhang, H.-Z.; Dong, Z.-Q. Novel Thin-Film Nanocomposite Membrane
428 with Water-Soluble Polyhydroxylated Fullerene for the Separation of Mg²⁺/Li⁺ Aqueous Solution.
429 *J Appl Polym Sci* **2019**, 48029. <https://doi.org/10.1002/app.48029>.

430 (11) Guo, C.; Qian, X.; Tian, F.; Li, N.; Wang, W.; Xu, Z. Amino-Rich Carbon Quantum Dots Ultrathin
431 Nanofiltration Membranes by Double “One-Step” Methods : Breaking through Trade-off among
432 Separation, Permeation and Stability. *Chemical Engineering Journal* **2021**, 404 (July 2020),
433 127144. <https://doi.org/10.1016/j.cej.2020.127144>.

434 (12) He, R.; Dong, C.; Xu, S.; Liu, C.; Zhao, S.; He, T. Unprecedented Mg²⁺/Li⁺ Separation Using Layer-
435 by-Layer Based Nanofiltration Hollow Fiber Membranes. *Desalination* **2022**, 525, 115492

436 (13) He, R.; Xu, S.; Wang, R.; Bai, B.; Lin, S.; He, T. Polyelectrolyte-Based Nanofiltration Membranes
437 with Exceptional Performance in Mg²⁺/Li⁺ Separation in a Wide Range of Solution Conditions. *J
438 Memb Sci* **2022**, 663, 121027.

439 (14) Li, H.; Wang, Y.; Li, T.; Ren, X. K.; Wang, J.; Wang, Z.; Zhao, S. Nanofiltration Membrane with
440 Crown Ether as Exclusive Li⁺ Transport Channels Achieving Efficient Extraction of Lithium from
441 Salt Lake Brine. *Chemical Engineering Journal* **2022**, 438, 135658.
442 <https://doi.org/10.1016/j.cej.2022.135658>.

443 (15) Zhang, T.; Zheng, W.; Wang, Q.; Wu, Z.; Wang, Z. Designed Strategies of Nanofiltration
444 Technology for Mg²⁺/Li⁺ Separation from Salt-Lake Brine: A Comprehensive Review. *Desalination*
445 **2023**, 546, 116205. <https://doi.org/10.1016/j.desal.2022.116205>.

446 (16) Wang, R.; He, R.; He, T.; Elimelech, M.; Lin, S. Performance Metrics for Nanofiltration-Based
447 Selective Separation for Resource Extraction and Recovery. *Nature Water* **2023**, 1, 291–300.
448 <https://doi.org/10.1038/s44221-023-00037-0>.

449 (17) Caus, A.; Braeken, L.; Boussu, K.; Van der Bruggen, B. The Use of Integrated Countercurrent
450 Nanofiltration Cascades for Advanced Separations. *Journal of Chemical Technology and*
451 *Biotechnology* **2009**, 84 (3), 391–398. <https://doi.org/10.1002/jctb.2052>.

452 (18) Hilal, N.; Kim, G. J.; Somer, C. Boron Removal from Saline Water : A Comprehensive Review.
453 *Desalination* **2011**, 273, 23–35. <https://doi.org/10.1016/j.desal.2010.05.012>.

454 (19) Caus, A.; Vanderhaegen, S.; Braeken, L.; Van der Bruggen, B. Integrated Nanofiltration Cascades
455 with Low Salt Rejection for Complete Removal of Pesticides in Drinking Water Production.
456 *Desalination* **2009**, 241 (1–3), 111–117. <https://doi.org/10.1016/j.desal.2008.01.061>.

457 (20) Jiang, C.; Chen, B.; Xu, Z.; Li, X.; Wang, Y.; Xu, T. Ion-“Distillation” for Isolating Lithium from Lake
458 Brine. *AIChE Journal* **2022**, 68, p.e17710. <https://doi.org/10.1002/aic.17710>.

459 (21) Wang, R.; Zhang, J.; Tang, C. Y.; Lin, S. Understanding Selectivity in Solute–Solute Separation:
460 Definitions, Measurements, and Comparability. *Environ Sci Technol* **2022**.
461 <https://doi.org/10.1021/acs.est.1c06176>.

462 (22) Yaroshchuk, A.; Bruening, M. L.; Eduardo, E.; Bernal, L. Solution-Diffusion-Electro-Migration
463 Model and Its Uses for Analysis of Nanofiltration, Pressure-Retarded Osmosis and Forward
464 Osmosis in Multi-Ionic Solutions. *J Memb Sci* **2013**, 447, 463–476.
465 <https://doi.org/10.1016/j.memsci.2013.07.047>.

466 (23) Yaroshchuk, A.; Bruening, M. L. An Analytical Solution of the Solution-Diffusion-Electromigration
467 Equations Reproduces Trends in Ion Rejections during Nanofiltration of Mixed Electrolytes. *J
468 Memb Sci* **2017**, 523, 361–372. <https://doi.org/10.1016/j.memsci.2016.09.046>.

469 (24) Yaroshchuk, A.; Bruening, M. L.; Zholkovskiy, E. Modelling Nanofiltration of Electrolyte Solutions.
470 *Adv Colloid Interface Sci* **2019**, 268, 39–63. <https://doi.org/10.1016/j.cis.2019.03.004>.

471 (25) Yaroshchuk, A. E. Negative Rejection of Ions in Pressure-Driven Membrane Processes. *Adv Colloid
472 Interface Sci* **2008**, 139 (1–2), 150–173. <https://doi.org/10.1016/j.cis.2008.01.004>.

473 (26) Labban, O.; Liu, C.; Chong, T. H.; Lienhard V, J. H. Fundamentals of Low-Pressure Nanofiltration:
474 Membrane Characterization, Modeling, and Understanding the Multi-Ionic Interactions in Water
475 Softening. *J Membr Sci* **2017**, *521*, 18–32. <https://doi.org/10.1016/j.memsci.2016.08.062>.

476 (27) Osorio, S. C.; Biesheuvel, P. M.; Dykstra, J. E.; Virga, E. Nanofiltration of Complex Mixtures : The
477 Effect of the Adsorption of Divalent Ions on Membrane Retention Layer. *Desalination* **2022**, *527*,
478 115552. <https://doi.org/10.1016/j.desal.2022.115552>.

479 (28) Li, Y.; Zhao, Y.; Wang, H.; Wang, M. The Application of Nanofiltration Membrane for Recovering
480 Lithium from Salt Lake Brine. *Desalination* **2019**, *468*, 114081.
481 <https://doi.org/10.1016/j.desal.2019.114081>.

482 (29) Foo, Z. H.; Rehman, D.; Bouma, A. T.; Monsalvo, S.; Lienhard, J. H. Lithium Concentration from
483 Salt-Lake Brine by Donnan-Enhanced Nanofiltration. *Environ Sci Technol* **2023**, *57* (15), 6320–
484 6330. <https://doi.org/10.1021/acs.est.2c08584>.

485

486

487

